

Reversible Transitions between Peptide Nanotubes and Vesicle-Like Structures Including Theoretical Modeling Studies

Xuehai Yan,^[a] Yue Cui,^[a] Qiang He,^[a, b] Kewei Wang,^[a] Junbai Li,^{*[a]} Weihua Mu,^[c] Bolin Wang,^[c] and Zhong-can Ou-yang^[c]

Abstract: Peptide-based self-assembling systems are increasingly attractive because of their wide range of applications in different fields. Peptide nanostructures are flexible with changes in the ambient conditions. Herein, a reversible shape transition between self-assembled dipeptide nanotubes (DPNTs) and vesicle-like structures is observed upon a change in the peptide

concentration. SEM, TEM, AFM, and CD spectroscopy were used to follow this transition process. We show that dilution of a peptide-nanotube dispersion solution results in the formation of

Keywords: nanotubes • peptides • reversible transitions • self-assembly • vesicle-like structures

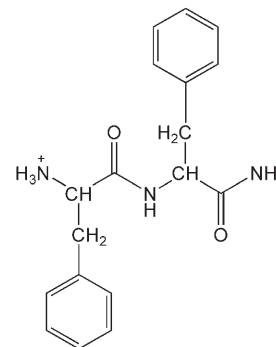
vesicle-like structures, which can then be reassembled into the nanotubes by concentrating the solution. A theoretical model describing this shape-transition phenomenon is presented to propose ways to engineer assembling molecules in order to devise other systems in which the morphology can be tuned on demand.

Introduction

Self-assembling systems based on peptides have important medical applications in bionanotechnology.^[1–5] For instance, the potential applications of biomaterials generated by novel synthetic peptides include scaffolding for tissue repair in regenerative medicine,^[6–10] biological surface engineering,^[11–15] drug delivery,^[16–18] and mimicking ion channels in biomembranes.^[19–25] Peptide nanostructures have been

shown to be flexible under changing experimental conditions. For example, the bola-amphiphile peptide monomer *N,N*-di-*p*-benzoic acid dodecane diacid diamide can be self-assembled into microspheres at pH 8 or nanotubes at pH 7 in citric acid/sodium hydroxide solutions, and a dumbbell-like intermediate can be obtained by switching the pH value between the spherical-growth and tubular-growth conditions.^[26] Moreover, Reches and Gazit showed that the introduction of a thiol group into the diphenylalanine peptide altered its assembly from tubular to spherical particles.^[27] In addition, Song et al. observed the change of self-assembled nanotubes of D-Phe–D-Phe dipeptides into vesicle-like structures when the peptide-nanotube (PNT) dispersion was diluted with water. Then, *NVT* (*N*: constant number of particles; *V*: volume; *T*: temperature) Monte Carlo simulations were performed to help the understanding of the self-assembly of the dipeptides.^[28] However, only a few theoretical models were established to explain the shape transition between the peptide nanotubes and spherical vesicle-like structures.

Previously, we reported that a cationic dipeptide (H-Phe–Phe-NH₂·HCl, **1**) can be self-assembled into nanotubes at physiological pH value and that



[a] Dr. X. Yan, Dr. Y. Cui, Dr. Q. He, Dr. K. Wang, Prof. J. Li
Beijing National Laboratory for Molecular Sciences (BNLMS)
International Joint Lab, Key Lab of Colloid and Interface Sciences
Institute of Chemistry
Chinese Academy of Sciences
Beijing 100080 (P. R. China)
Fax: (+86) 10-8261-2629
E-mail: jbli@iccas.ac.cn

[b] Dr. Q. He
Max Planck Institute of Colloids and Interfaces
14476 Golm/Potsdam (Germany)

[c] Dr. W. Mu, Dr. B. Wang, Prof. Z.-c. Ou-yang
Institute of Theoretical Physics
Chinese Academy of Sciences
Beijing 100080 (P. R. China)

Supporting information for this article is available on the WWW under <http://www.chemeurj.org/> or from the author. It contains SEM images of cationic-dipeptide nanotubes (calcd concentration of 8 mg mL⁻¹) concentrated from a 1 mg mL⁻¹ solution, an XRD diffractogram, and a figure depicting the two existing states of the dipeptide assemblies.

the resulting PNTs are spontaneously transformed into vesicle-like structures by diluting the PNT solution.^[29] Herein, we find that these peptide vesicle-like structures can be changed back into nanotubes by concentrating the diluted solution. That is, the transition between the dipeptide nanotubes (DPNTs) and vesicle-like structures is a reversible process which can be controlled by changing the peptide concentration. In addition, a theoretical model has been derived to help the understanding of the transition between the peptide nanotubes and vesicle-like structures.

Results and Discussion

Transition of DPNTs into vesicle-like structures: The cationic DPNTs were synthesized at a concentration of 10 mg mL^{-1} according to methods reported previously.^[29,30] SEM and TEM images confirmed the existence of the tubular structures self-assembled from cationic dipeptides (Figure 1a,b). As observed previously, the change of the assem-

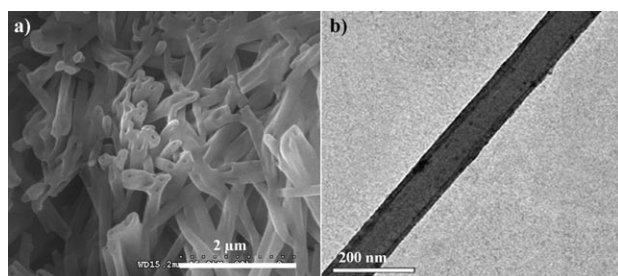


Figure 1. a) SEM image of the cationic DPNTs. b) TEM image of a cationic DPNT with staining by uranyl acetate aqueous solution.

bled nanostructures occurs when the DPNT dispersion solution is diluted with a phosphate-buffered saline (PBS) solution at pH 7.2. The transition from cationic DPNTs to vesicle-like structures started at a concentration of approximately 7 mg mL^{-1} and was complete at a concentration of 1 mg mL^{-1} .^[29] Therefore, when the cationic DPNT dispersion solution was diluted to 1 mg mL^{-1} , structural analysis by using TEM revealed that the cationic DPNTs had rearranged to form peptide vesicle-like structures (Figure 2a). Analysis by AFM confirmed the spherical shape of the nanostructures. These vesicle-like structures are approximately 50–100 nm in height, which is in line with the TEM analysis (Figure 2b). Furthermore, the dynamic transition process of the nanotubes into vesicle-like structures was recorded by using a fluorescence microscope equipped with a CCD camera (see the movie in the Supporting Information). At the beginning, the DPNTs (10 mg mL^{-1}) were labeled fluorescently by binding, through electrostatic interactions, with negatively charged single-stranded DNA (ss-DNA) with attached 5-((5-aminopentyl)thioureidyl)fluorescein (Figure 3a). Subsequently, the fluorescent nanotubes were diluted to 5 mg mL^{-1} . In addition to the DPNTs, a number of vesicle-like structures were also observed after a few sec-

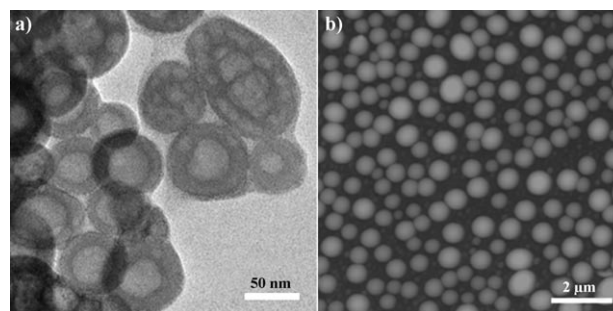


Figure 2. a) TEM image of the vesicle-like structures from cationic DPNTs when the DPNT dispersion solution was diluted to 1 mg mL^{-1} (with staining by uranyl acetate). b) Height image acquired by AFM for the vesicle-like structures from cationic DPNTs (z scale: 300 nm; height of vesicle-like structures: 50–100 nm).

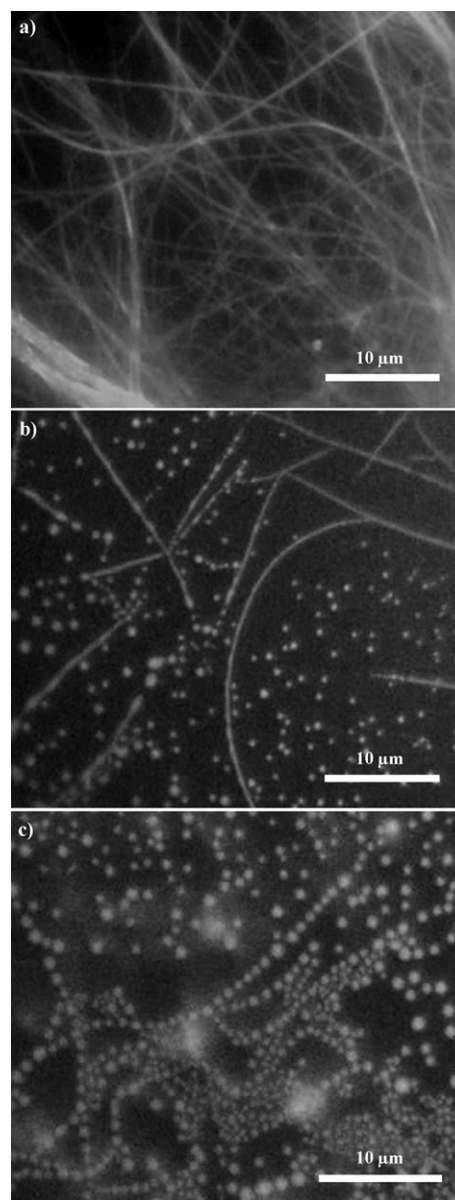


Figure 3. Fluorescence images of a) DPNTs with bound fluorescently labeled ss-DNA, b) the coexistence state of DPNTs and vesicle-like structures, and c) the joined necklace-like structures.

onds (Figure 3b). Then, all of the tubular structures were quickly converted into the vesicle-like structures. Moreover, necklace-like structures can be observed (Figure 3c). It should be noted that the fluorescently labeled ss-DNA promotes the transition from the nanotubes to the vesicle-like structures and makes the transition process easier to observe. This is likely because negative ss-DNA counteracts the partial positive charge on the surface of the DPNT or vesicle-like structure and further stabilizes the structure.

Reassembly of vesicle-like structures into DPNTs: After observing the transition of DPNTs into vesicle-like structures, we attempted to transform the vesicle-like structures to tubular structures by concentrating the diluted solution. As expected, we found that a large number of peptide nanotubes were reformed when the diluted cationic vesicle-like structures were concentrated to 8 mg mL^{-1} (see Figure S1a in the Supporting Information). An SEM image with a larger magnitude indicates a typical cationic-dipeptide tubular structure (see Figure S1b in the Supporting Information). Furthermore, a TEM image (Figure 4a) shows the tubular struc-

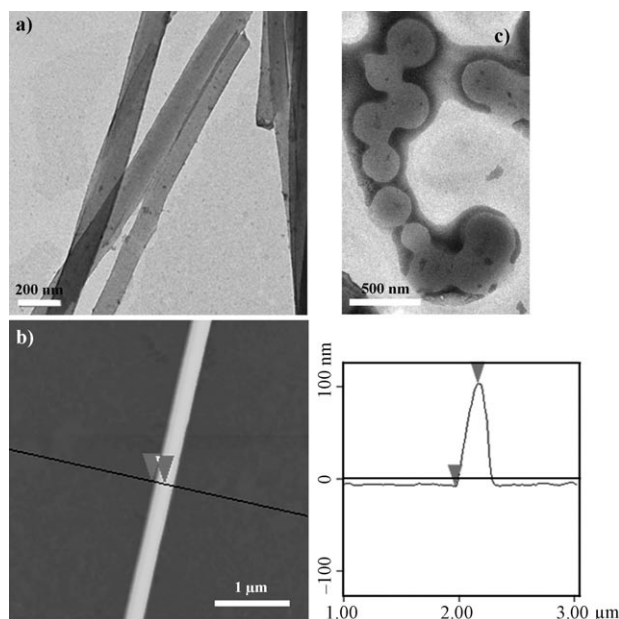


Figure 4. a) TEM image of the cationic DPNTs (calcd: 8 mg mL^{-1}) concentrated from a 1 mg mL^{-1} solution. b) Height AFM image of a cationic DPNT ($4 \times 4 \mu\text{m}$). The adjacent cross-sectional profile of the nanotube reveals its diameter to be 110 nm. c) TEM image of the joined necklace-like structure when the diluted peptide solution was concentrated to 6 mg mL^{-1} (calcd).

tures with enough contrast to distinguish the inner part and the periphery of the tube. An AFM image of the concentrated cationic-dipeptide sample reveals the three-dimensional topographic structure (Figure 4b). The cationic DPNTs are about 110 nm in height, as estimated from the cross-sectional profile. These analyses are consistent with the characteristics of the self-assembled DPNTs at 10 mg mL^{-1} . Additional-

ly, joined vesicles with a necklace-like structure were observed when the solution was concentrated to 6 mg mL^{-1} (calcd; Figure 4c). These results indicate that the concentration of peptide is a critical factor during the self-assembly of the peptide nanostructure and it affects the morphology of the self-assembled nanostructure. Thus, the peptide nanostructure morphology can be controlled by adjusting the concentration of the peptide.

CD measurements with the assembled DPNTs at 10 mg mL^{-1} showed a spectrum analogous to those of α -helical polypeptides (Figure 5a, spectrum 1). Indeed, the maximum at 192 nm and the minimum at 206 nm correspond to the α -helix π - π^* transition. The other absorption peak at 232 nm could correspond to n - π^* transitions of helical arrangements of the DPNTs.^[29,31] The vesicle-like-structure system did not show any obvious CD signal (Figure 5a, spectrum 2). The nanotubes reversely formed by concentrating the diluted solution showed a secondary structure similar to one of the assembled DPNTs at 10 mg mL^{-1} (Figure 5a, spectrum 3), which indicates that the peptide nanotubes were reassembled from the diluted solution. The change in turbidity was also measured when the nanotubes or vesicle-like structures were diluted or concentrated (Figure 5b). It can be seen that the turbidity decreases when the nanotube concentration is reduced (■ in Figure 5b), whereas the turbidity increases when the solution of vesicle-like structures is concentrated (● in Figure 5b). This result indicates that the reversible tube-to-vesicle-like morphological changes may occur during the changes in peptide concentration. It should be noted that the turbidity changes are different during dilution and concentration, which indicates hysteresis during the morphological changes. The TEM morphological analysis also shows that large numbers of vesicle-like structures, and a few nanotubes, can be observed when the diluted solution is concentrated to 6 mg mL^{-1} (calcd; Figure 5c).

Proposed self-assembly mechanism: It can be postulated that the driving force for the self-assembly of the dipeptides is offered by hydrogen bonding and π - π interactions, which are attractive forces between π electrons in the aromatic rings of dipeptides. The two existing states of the dipeptide assemblies are shown in Figure S2 in the Supporting Information. At the higher concentration of peptide (10 mg mL^{-1}), sufficient free energy of association by the intermolecular interactions can be gained. The aromatic residues in the peptide molecules consequently generate a three-dimensional aromatic-stacking arrangement that serves as a “glue” between the hydrogen-bonded cylinders of the peptide main chain and promotes nanotube formation.^[32] It should be noted that the X-ray diffractogram pattern of a cationic DPNT is slightly different to that of a diphenylalanine peptide nanotube (see Figure S3 in the Supporting Information).^[32] This is likely because the dipeptide charge state and the nature of the counterions that are eventually presented affect the molecular arrangements of the cationic dipeptide to some extent. However, both the hydrogen bonding and the π - π stacking governing the self-assem-

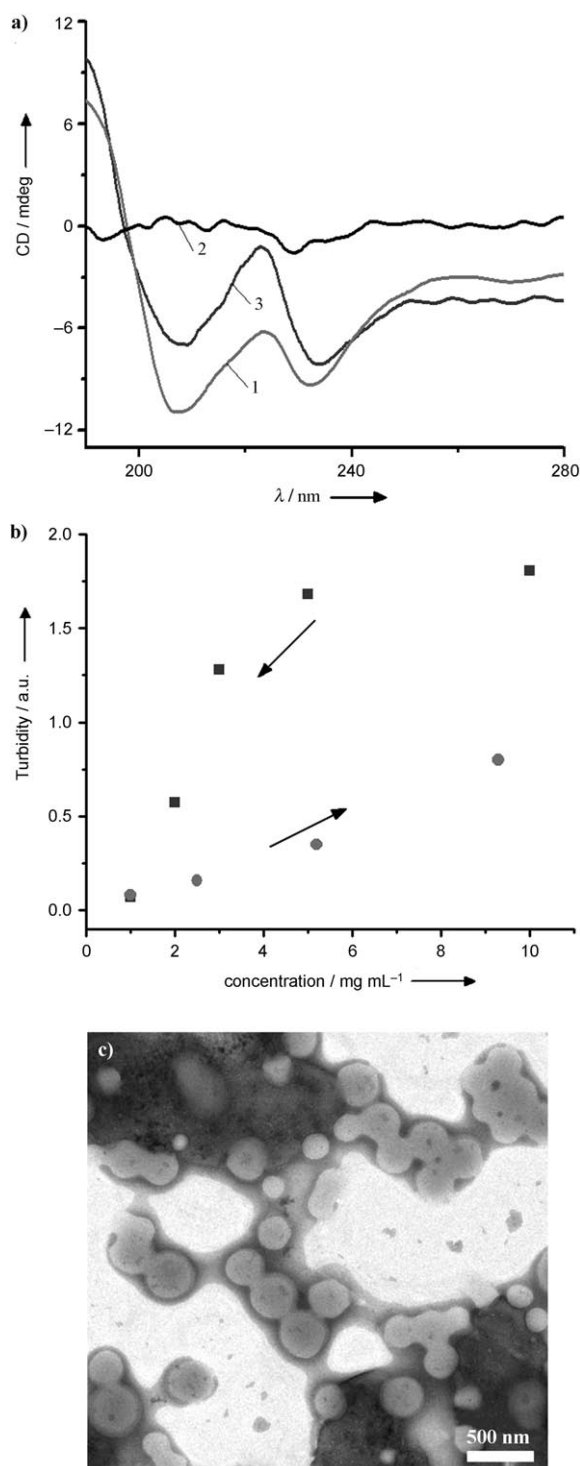


Figure 5. a) CD spectra of the cationic DPNTs and vesicle-like structures. 1: the self-assembled nanotubes at 10 mg mL^{-1} ; 2: vesicle-like structures at 1 mg mL^{-1} ; 3: the nanotubes after concentration of the diluted solution. b) Changes in turbidity with dilution (■) or concentration (●) of the peptide dispersion solution. c) TEM image of the vesicle-like structures when the diluted peptide solution was concentrated to 6 mg mL^{-1} (calcd).

bly process are deemed to be still valid in the cationic DPNT system. When the concentration of the peptide is decreased, the compact stacking structure of the nanotube is

broken and relatively noncompact stacking vesicle-like structures are rapidly formed by peptide reassembly. In particular, the necklace-like structure can be observed directly during concentration of the peptide dispersion system. This observation suggests that the joined vesicle-like structures may be precursors to the nanotubes. Similar to the results of the simulations performed by Song et al.,^[28] the dipeptide molecule behaves somewhat like a surfactant; the polar groups segregate from the hydrophobic phenyl groups to form bilayers, and some of the structures and continuous phases formed are similar to surfactant assemblies. In our experiment, the nanotubes are more likely to be composed of multilamellar or bicontinuous phases because they have thick tubular walls (see Figure 1a,b).

Theoretical model: Based on the above multilamellar model, we set up a model for the concentration-induced transition of the dipeptide nanotubes into spherical vesicle-like structures. The following model allows us to simulate the transition from the formation of multilamellar structures into other soft matters, such as the focal conical domains in smectic-A liquid crystals (LCs)^[33,34] or coils in multishell carbon nanotubes.^[35] As shown in reference [31], through the outward growth upon addition of a layer of thickness d on the top of the outermost equilibrium dipeptide aggregate (nanotube or vesicle-like structure), the corresponding increase in the interfacial area (A) and volume (V) for the multilamellar aggregate can be expressed by Equations (1) and (2), respectively, in which H and K are the mean curvature and the Gaussian curvature of the outer surface of the nanotube or vesicle-like structure, respectively.

$$\partial A = \oint (-2dH + d^2K) dA \quad (1)$$

$$\partial V = \oint (d - dH^2 + \frac{1}{3}d^3K) dA \quad (2)$$

The extra interfacial free energy is $\partial F_A = \gamma dA$, in which γ is the tension of the solution/aggregate interface. To form the layer, the association of dipeptide molecules from the solution (S) phase to the aggregate (A) phase induces a bulk free-energy variation of $\partial F_V = -g_0 \partial V$, in which g_0 is the Gibbs free-energy density between the S and A phases. Since the molecular entropy in the S phase is larger than that in the A phase, the g_0 value is positive and can be estimated with the ideal gas model through Equation (3), in which C_A and C_S are the concentrations (molecule number per volume) of dipeptide in the A and S phases, respectively, k_B is the Boltzman constant, and T is the temperature.

$$g_0 = C_A k_B T \ln(C_A/C_S) \quad (3)$$

In addition to these energy components, the extra growth costs a curvature elastic energy [Eq. (4)].^[36,37]

$$\partial F_C = (k_{11}d/2) \oint (2H)^2 dA + k_5 d \oint K dA \quad (4)$$

in which k_{11} is the splay elastic constant to the normal of the

layer (the director in LCs), and for $k_5=2k_{13}-k_{22}-k_{24}$, see the definitions in the Oseen–Frank elastic constants in LCs. The net free energy of growth is then given by Equation (5).

$$F = \partial F_C + \partial F_A + \partial F_V \quad (5)$$

$$= \oint [(-g_0/3)Kd^3 + (g_0H + \gamma K)d^2 + (2k_{11}H^2 + k_5K - g_0 - 2\gamma H)d]dA$$

The equilibrium shape of the aggregate can be obtained by $\partial F/\partial d=0$, that is, by Equation (6).

$$2k_{11}H^2 + k_5K - g_0 - 2\gamma H = 0 \quad (6)$$

It is then found that spheres (vesicle-like structures) of radius r_0 and cylinders (nanotubes) of radius ρ_0 are the solutions of Equation (6) if they satisfy the conditions in reference [33] [Eq. (7) and (8)].

$$r_0 = k/[(\gamma^2 + g_0k)^{1/2} - \gamma] \quad (7)$$

in which $k = 2k_{11} + k_5$

$$\rho_0 = k_{11}/[(\gamma^2 + 2k_{11}g_0)^{1/2} - \gamma] \quad (8)$$

The challenge is now to ask which shape would be preferred for a given C_A value, considering Equations (9) and (10).

$$(\gamma^2 + g_0k)^{1/2} - \gamma \approx kg_0/2\gamma \quad (9)$$

$$(\gamma^2 + 2k_{11}g_0)^{1/2} - \gamma \approx k_{11}g_0/\gamma \quad (10)$$

The above approximation of the series expansion is based on the experimental measurement in a liquid crystal of octyloxycyanobiphenyl (8OCB),^[33] for which $\gamma = 10^{-2} \text{ mNm}^{-1}$, $k_{11} = 10^{-11} \text{ N}$, and $g_0 = 4 \text{ Nm}^{-2}$. In the present peptide system, $\gamma = 5.63 \text{ mNm}^{-1}$ (see below), which guarantees the series development to be a better approximation than that in liquid crystals. Considering $H = -1/r_0$, $K = 1/r_0^2$ for spheres and $H = -1/2\rho_0$, $K = 0$ for tubes, substitution of Equations (7) and (8) into Equation (5) yields the growth energies for a unit area of a spherical vesicle-like-structure layer and a tube layer, which are $F_{\text{sphere}} = -(g_0^3d^3/12\gamma^2 + g_0^2d^2/4\gamma)$ and $F_{\text{tube}} = -g_0^2d^2/2\gamma$, respectively. We then find the condition for transition from a tube to a spherical vesicle-like structure to be $F_{\text{tube}} > F_{\text{sphere}}$, that is, $g_0d > 3\gamma$. By substituting $g_0d = 3\gamma$ into Equation (3), we obtained the critical tube-to-vesicle-like-structure concentration (CTVC) [Eq. (11)].

$$\text{CTVC} = C_A e^{-3\gamma/C_A d k_B T} \quad (11)$$

As $C_5 < \text{CTVC}$, nanotubes must transform into spherical vesicle-like structures rapidly. This confirms our above observation: the nanotubes can rapidly change into necklace-like structures during the dilution (Figures 3c and 4c; see also the movie in the Supporting Information). Here, for a given material, C_A has a constant value. For the cationic di-

peptide system this is given by Equation (12), in which D is the density of the cationic dipeptide in phase A and M_0 is the dipeptide molecular weight.

$$C_A = D/M_0 = 1.3 \times 10^6 \text{ g m}^{-3} / 363.5 \text{ g mol}^{-1} = 3.58 \times 10^3 \text{ mol m}^{-3} \quad (12)$$

From previous experimental information, we know that the transition of peptide nanotubes into vesicle-like structures starts at approximately $C_5 = 7 \text{ mg mL}^{-1}$ (19.26 mol m^{-3}). The d value is around 0.5 nm. Therefore, we can obtain a value of $\gamma = 5.63 \text{ mNm}^{-1}$ by substituting all of the values in Equation (11). The value of γ lies in the range of surface energies given in Table XV II in reference [38] for a series of materials and, particularly, is in very good agreement with the theoretically calculated values (in the range 3–6 mNm^{-1}). Moreover, the metastable necklace-like structures can be interpreted by the above theory. Indeed, as discussed in reference [33], if the k_5 value is ignored, the solution of Equation (6) is a surface with a constant mean curvature. In 1841, Delaunay^[39] found the following beautiful way to construct a rotationally symmetric hypersurface with a constant mean curvature: by rolling a given conical section on a straight line in a plane and then rotating the trace of a focus about the line, one obtains such a surface. Herein, the conical section is assumed to be an ellipse. A beaded structure is obtained by the Delaunay construction with a thin ellipse section (Figure 6a). If the ellipse is very wide, then the beaded

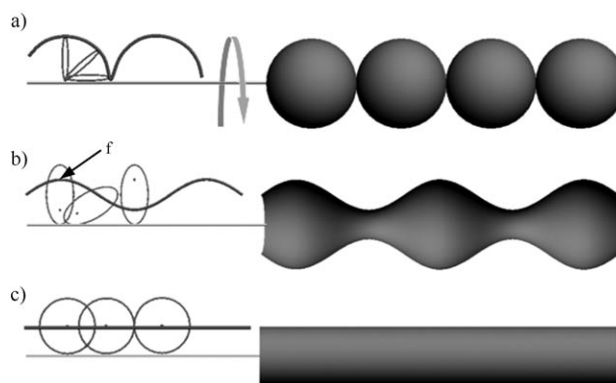


Figure 6. Illustration of the construction of a) a sphere, b) a necklace-like structure, and c) a tube with constant mean curvature by Delaunay's method. f is the focus of an ellipse.

structure becomes vesicles in a necklace-like structure (Figure 6b). At the other limit, if the ellipse becomes a circle, the resulting surface is a cylindrical tube (Figure 6c). In our experiments (Figure 3; see also the movie in the Supporting Information), by varying the C_5 value of the dipeptide, we obtained all of these shape transitions.

The agreement between the theoretical model and our experimental data again confirms that the model can serve for the description of the morphology of liquid crystals,^[33,34]

carbon nanotubes,^[35] and now peptide systems. In other words, the present model proposes a way to engineer assembling molecules, in order to devise other systems whose morphology could be tuned on demand. In order to devise peptide nanostructures, there are two ways to control the resulting structures. 1) For a given assembling molecule, at the same experimental temperature, both C_A and d are constant values, and thus CTVC is a function of the tension of the solution/aggregate interface (γ). The increase or decrease of the concentration of the assembling molecules will give a critical concentration at a specific γ value, which corresponds to the nanotubes or spherical vesicle-like structures. 2) When we select or design assembled peptide molecules with different architectures,^[9,26–28,40,41] which will have different hydrophobic/hydrophilic properties, the values of γ and the molecular size (d) will change correspondingly [Eq. (11)] and will thus give a new critical concentration for the transition on demand.

Finally, we would like to point out that there is still room to improve the above theoretical model^[42] by incorporating the bulk energy of the molecules in the solution into the free energy value, F_v . This term may be an important parameter in the shape transition of the peptide-based self-assembling systems. Currently, only the entropy is included in the F_v value. This is due to the consideration that for many hydrocarbons (for example, benzene), the entropy contribution to the g_0 value is even higher and closer to the range of 85–100% (see page 104 in reference [38]).

Conclusion

It has been found that the cationic dipeptide is first assembled into nanotubes at higher concentrations, and these tubular structures can spontaneously be converted into vesicle-like structures at lower concentrations. This reversible transition process is important for understanding the molecular self-assembly of diphenylalanine, the core recognition motif of the Alzheimer's β -amyloid polypeptide, and may contribute to a deeper understanding of the molecular mechanism of protein misfolding. Based on the reversible shape transition between DPNTs and vesicle-like structures, we have presented an equation, which has not been reported before, to demonstrate the rationality of the shape transitions in combination with Delaunay's construction method. The theoretical model can also be used to differentiate the shape of the aggregate phase in solution. Additionally, the γ value, which is the tension of the solution/aggregate interface, can be calculated if the CTVC value was determined through the experiment. Therefore, the theoretical model of the CTVC value has critical significance in helping the understanding of some shape-transition phenomena in molecular self-assembly.

Experimental Section

Materials and methods: The cationic dipeptide (H-Phe-Phe-NH₂-HCl) was purchased from Bachem (Bubendorf, Switzerland). The cationic DPNTs were self-assembled by dissolving dipeptide (10 mg) in 1,1,1,3,3,3-hexafluoro-2-propanol (HFP; 80 μ L; Sigma-Aldrich) and then diluting this mixture into a 10 mg mL⁻¹ aqueous solution with PBS solution (460 μ L; pH 7.2) or NH₃·H₂O (460 μ L; pH 7.8). The concentration process was as follows: A 2 mL homopolymer microtube containing the 1 mg mL⁻¹ dispersion solution of the assembled peptide structure was placed in a desiccator and the solvent was allowed to evaporate. Samples were taken out at different times to calculate the concentration of the dispersion system and for measurements.

Microscopy: The SEM images were acquired by an S-4300 microscope (Hitachi, Japan). TEM was carried out with a Philips CM200-FEG instrument. The movie was recorded by using an Olympus IX-70 fluorescence microscope equipped with a CCD camera. The AFM images were recorded with a Nanoscope IIIa instrument (Digital Instruments, Veeco Metrology Group, Santa Barbara, CA) in tapping mode in air. Aliquots (5–10 μ L) of peptide nanotubes or vesicle-like structures were pipetted onto the surface of freshly cleaved mica, left for a few minutes, and then dried with a gentle stream of nitrogen. XRD data for cationic DPNTs prepared in pure water were collected at 3–50° by using a Rigaku D/max-2500 instrument (Cu_{K α}).

CD spectra: CD spectra were recorded in a JASCO 810 spectrometer at room temperature between 190 and 280 nm by taking points at 1 nm, with an integration time of 0.5 s. Data were collected with peptide samples on a quartz chip at a scan speed of 25 nm min⁻¹ with 0.5 nm step size. Each spectrum was the average of four measurements.

Turbidity measurements: Turbidity was measured by a U-3010 UV/Visible spectrometer (Hitachi) with UV/Vis Chem Station software. The measurements were carried out at a wavelength of 500 nm, at which value the absorption of the aggregates was minimized. The diluting or concentrating samples were left for more than an hour before measurements were taken.

Fluorescence microscopy: An assembled DPNT (10 mg mL⁻¹) was labeled fluorescently by binding with negatively charged ss-DNA labeled with 5-((5-aminopentyl)thioureidyl)fluorescein through electrostatic interactions. The above DPNT dispersion solution was diluted to 5 mg mL⁻¹. An aliquot (5 μ L) was then immediately pipetted onto a microscope glass cover slip and observed by using an Olympus IX-70 fluorescence microscope equipped with a CCD camera.

Acknowledgement

We acknowledge financial support of this research by the National Basic Research Program of China (973 program; grant no.: 2007CB935900), the Chinese Academy of Sciences (grant no.: KJXC2-SW-H12), and the German Max-Planck Society. Q.H. is grateful to the Alexander von Humboldt Foundation for a research fellowship.

- [1] S. Zhang, *Nat. Biotechnol.* **2003**, *21*, 1171–1178.
- [2] X. Y. Gao, H. Matsui, *Adv. Mater.* **2005**, *17*, 2037–2050.
- [3] D. T. Bong, T. D. Clark, J. R. Granja, M. R. Ghadiri, *Angew. Chem.* **2001**, *113*, 1016–1041; *Angew. Chem. Int. Ed.* **2001**, *40*, 988–1011.
- [4] C. Valery, M. Paternostre, B. Robert, T. Gulik-Krzywicki, T. Narayanan, J. C. Dedieu, G. Keller, M. L. Torres, R. Cherif-Cheikh, P. Calvo, F. Artzner, *Proc. Natl. Acad. Sci. USA* **2003**, *100*, 10258–10262.
- [5] A. Aggeli, I. A. Nyrkova, M. Bell, R. Harding, L. Carrick, T. C. B. McLeish, A. N. Semenov, N. Boden, *Proc. Natl. Acad. Sci. USA* **2001**, *98*, 11857–11862.
- [6] J. D. Hartgerink, E. Beniash, S. I. Stupp, *Science* **2001**, *294*, 1684–1688.

- [7] G. A. Silva, C. Czeisler, K. L. Niece, E. Beniash, D. A. Harrington, J. A. Kessler, S. I. Stupp, *Science* **2004**, *303*, 1352–1355.
- [8] T. C. Holmes, S. de Lacalle, X. Su, G. Liu, A. Rich, S. Zhang, *Proc. Natl. Acad. Sci. USA* **2000**, *97*, 6728–6733.
- [9] J. Kisiday, M. Jin, B. Kurz, H. Hung, C. Semino, S. Zhang, A. J. Grodzinsky, *Proc. Natl. Acad. Sci. USA* **2002**, *99*, 9996–10001.
- [10] K. Rajangam, H. A. Behanna, M. J. Hui, X. Han, J. F. Hulvat, J. W. Lomasney, S. I. Stupp, *Nano Lett.* **2006**, *6*, 2086–2090.
- [11] E. Beniash, J. D. Hartgerink, H. Storrie, J. C. Stendahl, S. I. Stupp, *Acta Biomaterialia* **2005**, *1*, 387–397.
- [12] S. Zhang, L. Yan, M. Altman, M. Lässle, H. Nugent, F. Frankel, D. A. Lauffenburger, G. M. Whitesides, A. Rich, *Biomaterials* **1999**, *20*, 1213–1220.
- [13] A. P. Nowak, V. Breedveld, L. Pakstis, B. Ozbas, D. J. Pine, D. Pochan, T. J. Deming, *Nature* **2002**, *417*, 424–428.
- [14] A. Mahler, M. Reches, M. Rechter, S. Cohen, E. Gazit, *Adv. Mater.* **2006**, *18*, 1365–1370.
- [15] V. Jayawarna, M. Ali, T. A. Jowitt, A. F. Miller, A. Saiani, J. E. Gough, R. V. Ulijn, *Adv. Mater.* **2006**, *18*, 611–614.
- [16] C. Keyes-Baig, J. Duhamel, S. Fung, J. Bezaire, P. Chen, *J. Am. Chem. Soc.* **2004**, *126*, 7522–7532.
- [17] T. Gore, Y. Dori, Y. Talmon, M. Tirrell, H. Bianco-Peled, *Langmuir* **2001**, *17*, 5352–5360.
- [18] E. Kokkoli, A. Mardilovich, A. Wedekind, E. L. Rexeisen, A. Garg, J. A. Craig, *Soft Matter*, **2006**, *2*, 1015–1024.
- [19] S. Fernandez-Lopez, H. S. Kim, E. C. Choi, M. Delgado, J. R. Granja, A. Khasanov, K. Kraehenbuehl, G. Long, D. A. Weinberger, K. M. Wilcoxon, M. R. Ghadiri, *Nature* **2001**, *412*, 452–455.
- [20] J. S. Quesada, M. P. Isler, M. R. Ghadiri, *J. Am. Chem. Soc.* **2002**, *124*, 10004–10005.
- [21] V. Percec, A. E. Dulcey, V. S. K. Balagurusamy, Y. Miura, J. Smidkhal, M. Peterca, S. Nummelin, U. Edlund, S. D. Hudson, P. A. Heiney, H. Duan, S. N. Maganov, S. A. Vinogradov, *Nature* **2004**, *430*, 764–768.
- [22] V. Percec, A. E. Dulcey, M. Peterca, M. Ilies, J. Ladislav, B. M. Rosen, U. Edlund, P. A. Heiney, *Angew. Chem.* **2005**, *117*, 6674–6679; *Angew. Chem. Int. Ed.* **2005**, *44*, 6516–6521.
- [23] V. Percec, A. E. Dulcey, M. Peterca, M. Ilies, S. Nummelin, M. J. Sienkowska, P. A. Heiney, *Proc. Natl. Acad. Sci. USA* **2006**, *103*, 2518–2523.
- [24] R. MacKinnon, *Angew. Chem.* **2004**, *116*, 4363–4376; *Angew. Chem. Int. Ed.* **2004**, *43*, 4265–4277.
- [25] P. Agre, *Angew. Chem.* **2004**, *116*, 4377–4390; *Angew. Chem. Int. Ed.* **2004**, *43*, 4278–4290.
- [26] H. Matsui, C. Holtman, *Nano Lett.* **2002**, *2*, 887–889.
- [27] M. Reches, E. Gazit, *Nano Lett.* **2004**, *4*, 581–585.
- [28] Y. J. Song, S. R. Challa, C. J. Medforth, Y. Qiu, R. K. Watt, D. Pena, J. E. Miller, F. van Swol, J. A. Shelnut, *Chem. Commun.* **2004**, 1044–1045.
- [29] X. Yan, Q. He, K. Wang, L. Duan, Y. Cui, J. Li, *Angew. Chem.* **2007**, *119*, 2483–2486; *Angew. Chem. Int. Ed.* **2007**, *46*, 2431–2434.
- [30] M. Reches, E. Gazit, *Science* **2003**, *300*, 625–627.
- [31] N. Berova, K. Nakanishi, R. W. Woody, *Circular Dichroism: Principles and Applications*, 2nd ed., Wiley-VCH, New York, **2000**.
- [32] C. H. Görbitz, *Chem. Commun.* **2006**, 2332–2334.
- [33] H. Naito, M. Okuda, Z. Ou-yang, *Phys. Rev. Lett.* **1993**, *70*, 2912–2915.
- [34] H. Naito, M. Okuda, Z. Ou-yang, *Phys. Rev. E* **1995**, *52*, 2095–2098.
- [35] Z. Ou-yang, Zhao-Bin Su, Chui-lin Wang, *Phys. Rev. Lett.* **1997**, *78*, 4055–4058.
- [36] W. Helfrich, *Z. Naturforsch C* **1973**, *28*, 693–703.
- [37] Z. Ou-yang, S. Liu, Xie Yu-Zhang, *Mol. Cryst. Liq. Cryst.* **1991**, *204*, 143–154.
- [38] J. N. Israelachvili, *Intermolecular and Surface Forces*, Academic Press, London, **1985**, p. 158.
- [39] C. Delaunay, *J. Math. Pures et Appliquées* **1841**, *1*, 309–320.
- [40] T. Shimizu, M. Masuda, H. Minamikawa, *Chem. Rev.* **2005**, *105*, 1401–1443.
- [41] S. Santoso, W. Hwang, H. Hartman, S. Zhang, *Nano Lett.* **2002**, *2*, 687–691.
- [42] This issue is raised in accordance with a valuable suggestion from a referee of our paper.

Received: January 4, 2008
Published online: May 14, 2008